Evidence for solar frequency dependence on sunspot type

Charles S. Baldner

Department of Astronomy, Yale University, P.O. Box 208101, New Haven, CT, 06520-8101

Richard S. Bogart

Hansen Experimental Physics Laboratory, Stanford University, Stanford, CA 94305-4085

and

Sarbani Basu

Department of Astronomy, Yale University, P.O. Box 208101, New Haven, CT, 06520-8101

January 20, 2013

ABSTRACT

High degree solar mode frequencies as measured by ring diagrams are known to change in the presence of the strong magnetic fields found in active regions. We examine these changes in frequency for a large sample of active regions analyzed with data from the Michelson Doppler Imager (MDI) onboard the SoHO spacecraft, spanning most of solar cycle 23. We confirm that the frequencies increase with increasing magnetic field strength, and that this dependence is generally linear. We find that the dependence is slightly but significantly different for active regions with different sunspot types.

Subject headings: Sun: activity, Sun: helioseismology

1. Introduction

Active regions are complex, dynamic objects and are prominent manifestations of solar activity. Understanding the nature, origin, and development of these regions is one of the most important outstanding questions in solar physics. Helioseismology provides us with a means to probe the layers of the Sun below the surface of active regions, and has the potential to yield important clues about their structure and evolution. In particular, helioseismology can give us information about the flows and dynamical structures associated with active

regions, about the depth and extent of thermal disturbances beneath sunspots and other surface phenomena, and about the nature of the magnetic fields that rise to form active regions.

The frequencies of global oscillations change with the overall level of solar activity (Woodard & Noyes 1985; Libbrecht & Woodard 1990); this is by now very well established (see review by Christensen-Dalsgaard 2002, and references therein). The frequencies of both low degree modes (e.g. Chaplin et al. 2007) and medium degree modes (e.g. Dziembowski et al. 1998; Howe et al. 1999; Dziembowski et al. 2000) increase with solar activity level, and this frequency increase is stronger at higher frequencies. Though high degree global mode measurements are not routinely made, some sets of high degree mode frequency measurements have been made, and these are found to increase with activity as well (Rabello-Soares & Korzennik 2009).

The use of so-called 'ring diagrams' (Hill 1988) to study solar structure is by now a well-established technique in helioseismology (see review by Gizon & Birch 2005). In this paper, we will discuss the changes to mode parameters in ring diagrams between active regions and the surrounding quiet Sun. Ring diagrams prove useful for studying the effects of solar activity on helioseismic modes for two reasons. First, rings are measured on a localized patch of the Sun, providing both temporal and spatial resolution. This allows us to isolate phenomena associated with solar activity from the surrounding Sun. Second, measurements can be made to much higher degree much more easily than with global mode analysis. Ring diagrams were first used by Hill (1988) to measure flow rates near the solar surface. Rings have been used subsequently by a number of authors to study the near-surface dynamics of the Sun (e.g. Schou & Bogart 1998; Basu et al. 1999; Haber et al. 1999). Ring diagrams have also been used to study the thermal structure beneath sunspots and in the near-surface layers (Basu et al. 2004, 2007; Bogart et al. 2008).

The effects of active regions on ring diagram mode parameters have been studied in previous works. Hindman et al. (2000) found that the high degree mode frequencies obtained from ring diagrams were enhanced in active regions. Rajaguru et al. (2001) found that the mode widths were also enhanced in active regions, while the amplitudes were suppressed, and Rabello-Soares et al. (2008) found that the relation between the change in width and mode amplitude was very nearly linear. Howe et al. (2004) assumed that the relation between activity and mode parameter variation was quadratic, and found a peak increase in mode frequency at around 5mHz, with a corresponding maximum change in width and amplitude.

In this work, we study the properties of 264 active region ring diagrams from solar cycle 23. This sample gives us a statistically significant number of measurements over a substantial range of activity levels from all phases of the solar cycle, when compared to earlier works.

2. Data

The data are resolved line-of-sight velocity measurements of the solar surface taken by the Michelson Doppler Imager (MDI) on board the *Solar and Heliospheric Observatory* (SOHO) spacecraft (Scherrer et al. 1995). Ring diagrams are constructed from small, $16^\circ \times 16^\circ$ patches of the solar disk, tracked to move with the solar differential rotation. The regions are tracked across the solar disk center. The observation cadence is 1 minute, and the patches are tracked for 8192 minutes. They are projected onto a rectangular grid using Postel's projection and corrected for the distortion in the MDI optics. The Doppler cubes are then Fourier transformed to obtain a three dimensional power spectrum. A more detailed discussion of the construction of ring diagrams can be found in Patron et al. (1997) and Basu et al. (1999).

The spectra are fit in the same way as Basu et al. (2004). The functional form is from Basu et al. (1999); it is an asymmetric Lorentzian profile with terms for advection in both transverse directions and for azimuthally asymmetric power distribution. Fits are done at constant frequency, so that to interpret these measurements as discrete normal modes, we interpolate along each ridge to integer values of the degree ℓ. Errors are treated in the same way as (Basu et al. 2004).

Target active regions are selected from the NOAA active region catalog. Ring diagrams require higher resolution Dopplergrams than the usual MDI 'medium-ℓ' data that are collected continuously. We use full-disk Dopplergram data which are one of MDI's 'high rate' data products, produced mainly during yearly two to three month dynamics run campaigns. We require a data coverage of greater than 80%. The NOAA active region catalog includes sunspot classifications according to the Mt. Wilson scheme. The Mt. Wilson classifications are α, β, γ, and δ, and combinations of these. The NOAA catalog lists active regions for each day that they are visible, and in the case where the classification changes, we take the classification closest to center disk crossing. In our sample, 90% of the active regions are classified as either α, which are unipolar groups, or β, which are simple bipolar groups.

Ring diagrams suffer from a number of systematic effects. These arise primarily from foreshortening when away from disk center, and secular changes in the characteristics of the MDI instrument. These effects can be minimized by studying the mode parameters of an active region relative to a quiet Sun region, tracked at the same latitude and as near in time as possible. For this sample, two quiet regions were chosen for each active region, one on either side of the active region.

In order to characterize the level of activity in our rings, we use a measure of the total unsigned line-of-sight magnetic flux. This measure is the Magnetic Activity Index (MAI),

which is described in Basu et al. (2004) and is a measure of the strong magnetic unsigned flux in the ring diagram aperture. In brief, the MAI is the spatial and temporal average of all MDI magnetogram pixels with a flux greater than 50G, taken over the same aperture and time range as the velocity data for the ring diagrams. The activity in each region, then, is characterized by a single number, and differential measurements can be characterized by the difference in MAI, $\Delta\,\mathrm{MAI}$, between the active region and the quiet comparison region. We also fit a linear trend in time to the spatial averages of the magnetograms. This gives a rough measure of the growth or decay of the active region, and we refer to this quantity as the growth parameter.

3. Analysis

Mode parameters for all rings and comparison regions were fit using the profile from Basu et al. (1999). We interpolate the ridge fits to integer values of ℓ, and take the differences in frequency $\delta\nu$. The sense of the differences are active minus quiet. In Figure 1, we show averages of the scaled frequency differences $\langle\delta\nu/\nu\rangle$ for the f-mode and the first three p-modes. The frequency ranges chosen have relatively small errors and were fit in most regions in the sample. The behavior seen in Figure 1 is nevertheless representative of the rest of the data in our sample. The majority of $\Delta\,\mathrm{MAI}$ values are fairly small — this is in part due to the fact that the majority of active regions do not have particularly large MAI values, but also due to the fact that, at high activity levels in particular, it is sometimes difficult to find a suitable quiet region for comparison. The comparison regions therefore sometimes have fairly significant MAI values.

We confirm earlier results finding that, in the presence of magnetic fields, helioseismic frequencies increase. We find that, for small and intermediate magnetic field strengths ($\Delta\,\mathrm{MAI} \lesssim 200$ G), the relationship is linear. For the p-mode differences, the correlation coefficients mostly range between 0.6 and 0.7. The f-mode frequencies have larger errors, and the correlation coefficients are correspondingly lower. The best fit linear regression lines are also shown. The reduced χ^2 values computed from the residuals are large — between 3 and 15 for sets of averages. Thus, the computed errors in the fitted frequencies do not completely account for the observed scatter in the frequency differences. It is possible that a linear relation does not completely account for the dependence of frequency on $\Delta\,\mathrm{MAI}$, but we have tested a variety of higher order polynomials and other functional forms without substantially reducing the χ^2 values. When fitting higher order polynomials, the best fits return essentially the same linear fits as shown in Figure 1, with negligibly small non-linear coefficients. Other functional forms generally increased the χ^2 values.

As a test of the assumption of linearity, we apply an Anderson-Darling test to the residuals from the linear best fits. The residuals from the linear regression fit fail an Anderson-Darling test at the 1% level. This implies either that the errors are non-gaussian, or that the relation between magnetic activity and shift in frequency is not entirely linear.

At high magnetic field strengths ($\Delta\,\mathrm{MAI} \gtrsim 200$ G), a visual inspection of Figure 1 might suggest a 'saturation' effect in the frequency shifts. Evidence for such an effect in thermodynamic perturbations beneath active regions has been suggested (Basu et al. 2004; Bogart et al. 2008). In this case, however, we do not find that the outliers at high field strengths are statistically significant. Fitting different slopes at low and high activity does not change the χ^2 values of the residuals, and removing the high activity regions from the sample does not substantially change either the χ^2 values or the Anderson-Darling A^2 statistic of the residuals. Further, we have tested whether or not the presence of some comparison regions with significant activity is introducing bias. We find that, when the sample is divided between quiet and moderately active comparison regions, the frequency differences are indistinguishable. It must be noted, however, that a saturation effect is not *inconsistent* with our data, either. A larger sample of high field strength regions will be required to adequately address this problem.

To show the behavior of the dependence of frequency on activity, we fit a straight line to each individual mode difference as a function of MAI:

$$\frac{\delta\nu_{n,\ell}}{\nu_{n,\ell}} = a_{n,\ell}\Delta\,\mathrm{MAI} + b_{n,\ell}. \tag{1}$$

The slopes $a_{n,\ell}$ are shown in Figure 2. The slopes in frequency shifts are seen to increase with frequency. It is notable, however, that the slopes are not a pure function of frequency — different n-ridges have slightly different dependences on frequency. At high frequency, there is some indication that the slopes turn over. It has been observed in MDI data (Howe et al. 2008) and in Helioseismic and Magnetic Imager (HMI) data (Howe et al. 2011) that for frequencies above the acoustic cutoff, the slopes of frequency with magnetic field strength do in fact become negative. In our own sample, however, the quality of the fits do not permit us to extend our work much beyond the acoustic cutoff.

We have examined the differences between different classes of sunspots in the centers of active regions. The majority of the active regions in our sample are classified as α or β types. When subdivided by type, the linear correlation is somewhat changed (though the correlation coefficients are not), and the distribution of the residuals for for the α-type active regions now satisfy an Anderson-Darling test for normality at the 15% level. The residuals for the β-type active regions do pass the 10% test, but do not do as well as the α-types. The slopes of the fits and the correlation coefficients are not changed by a statistically significant

amount. In Figure 3 we show examples of $\langle \delta\nu \rangle$ separated by active region type, and the residuals to a linear fit.

The differences in the slopes between the α-type regions and the β-type regions are shown in Figure 4. There is a small but systematic trend with frequency in the slopes. For $\nu \lesssim 3.5$ mHz, α-type spots have very slightly smaller slopes $a_{n,\ell}$, while they are slightly larger for modes with $\nu > 3.5$ mHz.

We have also subdivided the sample in a number of different ways to attempt to determine if the mode parameters are sensitive to other variables than the total magnetic field strength in the region. The fitted parameters were checked for secular trends with time, or for any dependencies on the latitude of the region. We have found no statistically significant differences in the mode parameters or their behavior with increasing activity, either as a function of time over solar cycle 23 or as a function of latitude. We can also split the sample in two using the growth parameter of the MAI as a rough measure of whether or not a given active region is growing or decaying. The statistical properties of these two sub-samples are indistinguishable from their parent sample. The confidence level for all of these claims is at the 95% level or greater.

4. Discussion

It is by now well established that helioseismic frequencies below the acoustic cutoff frequency are enhanced in the presence of magnetic fields. In this work, we have measured mode frequencies for a large sample of active regions using ring diagram analysis. We find, consistent with most earlier work, that shifts in frequency are linearly correlated with the magnetic activity measured at the surface. These correlations hold for all mode sets and for the whole range of frequencies studied.

Both Howe et al. (2004) and Rabello-Soares et al. (2008) have presented frequency shifts with ring diagrams at various levels of magnetic activity. Our results are generally quantitatively consistent with theirs, though we do not find any evidence of a quadratic dependence of the mode parameters on activity, as Howe et al. (2004) did. Rabello-Soares et al. (2008) find what appears to be a much cleaner relation with frequency than we do, in spite of the fact that they use the same frequency fitting technique and data from the same instrument. This is most likely due to the much smaller number of regions used in that study.

Our finding that the helioseismic frequencies of different active region types may be drawn from different statistical populations is novel, but it is not immediately clear what the significance of this result is. It implies that the surface geometry, not only strength, of

the magnetic fields in an active region may determine the oscillation characteristics of the Sun.

It has been shown that the inclination of the magnetic fields can affect the amount of acoustic power absorption (e.g. Cally et al. 2003). Observational evidence for this has been found using helioseismic holography (Schunker et al. 2005, 2008) and time-distance analysis (Zhao & Kosovichev 2006). It is possible that we are seeing this effect averaged out over the much larger region sampled in ring diagram analysis.

Although we do find that the slopes $a_{n,\ell}$ are slightly different for the two different active region types, the fact that these differences appear to be simply a function of frequency implies that it is very unlikely do be due to changes in the thermal structure in the regions typically resolved in ring diagram structure inversions. In the region where the upper turning points of the modes are located, however, it is possible that a different thermal stratification in different sunspot types would give rise to a difference such as the one we have detected, since upper turning points are shallower with increasing frequency. The direct effects of magnetic fields also have an effect on the upper turning points, as was shown by Jain (2007) in the case of horizontal magnetic fields.

The errors in the measurement of the MAIs are small, but it is possible that small systematic errors arise from the fact that the calculation is restricted to the line-of-sight fields. Different surface field configurations could give rise to somewhat different systematic errors. It is difficult to estimate how large this effect could be at present, but continuously available high-resolution data becoming available from the Helioseismic and Magnetic Imager (HMI) on the Solar Dynamics Observatory (SDO) is allowing full vector inversions for magnetic fields. This will allow us to more accurately compute the total magnetic fields in active regions.

CSB is supported by a NASA Earth and Space Sciences fellowship NNX08AY41H. SB is supported by NSF grants ATM 0348837 and ATM 0737770 to SB. This work utilizes data from the Solar Oscillations Investigation/ Michelson Doppler Imager (SOI/MDI) on the Solar and Heliospheric Observatory (SOHO). SOHO is a project of international cooperation between ESA and NASA. MDI is supported by NASA grants NAG5-8878 and NAG5-10483 to Stanford University.

REFERENCES

Basu, S., Antia, H. M., & Bogart, R. S. 2004, ApJ, 610, 1157

Basu, S., Antia, H. M., & Bogart, R. S. 2007, ApJ, 654, 1146

Basu, S., Antia, H. M., & Tripathy, S. C. 1999, ApJ, 512, 458

Bogart, R. S., Basu, S., Rabello-Soares, M. C., & Antia, H. M. 2008, Sol. Phys., 251, 439

Cally, P. S., Crouch, A. D., & Braun, D. C. 2003, MNRAS, 346, 381

Chaplin, W. J., Elsworth, Y., Miller, B. A., Verner, G. A., & New, R. 2007, ApJ, 659, 1749

Christensen-Dalsgaard, J. 2002, Reviews of Modern Physics, 74, 1073

Dziembowski, W. A., Goode, P. R., di Mauro, M. P., Kosovichev, A. G., & Schou, J. 1998, ApJ, 509, 456

Dziembowski, W. A., Goode, P. R., Kosovichev, A. G., & Schou, J. 2000, ApJ, 537, 1026

Gizon, L., & Birch, A. C. 2005, Living Reviews in Solar Physics, 2, 6

Haber, D. A., Hindman, B. W., Toomre, J., Bogart, R. S., Schou, J., & Hill, F. 1999, SOHO-9 Workshop on Helioseismic Diagnostics of Solar Convection and Activity, 9,

Hindman, B., Haber, D., Toomre, J., & Bogart, R. 2000, Sol. Phys., 192, 363

Hill, F. 1988, ApJ, 333, 996

Howe, R., Komm, R., & Hill, F. 1999, ApJ, 524, 1084

Howe, R., Komm, R. W., Hill, F., Haber, D. A., & Hindman, B. W. 2004, ApJ, 608, 562

Howe, R., Haber, D. A., Hindman, B. W., Komm, R., Hill, F., & Gonzalez Hernandez, I. 2008, Subsurface and Atmospheric Influences on Solar Activity, 383, 305

Howe, R., Tripathy, S., González Hernández, I., Komm, R., Hill, F., Bogart, R., & Haber, D. 2011, Journal of Physics Conference Series, 271, 012015

Jain, R. 2007, ApJ, 656, 610

Libbrecht, K. G., & Woodard, M. F. 1990, Nature, 345, 779

Patron, J., et al. 1997, ApJ, 485, 869

Rabello-Soares, M. C., & Korzennik, S. G. 2009, Astronomical Society of the Pacific Conference Series, 416, 277

Rabello-Soares, M. C., Bogart, R. S., & Basu, S. 2008, Journal of Physics Conference Series, 118, 012084

Rajaguru, S. P., Basu, S., & Antia, H. M. 2001, ApJ, 563, 410

Scherrer, P. H., et al. 1995, Sol. Phys., 162, 129

Schou, J., & Bogart, R. S. 1998, ApJ, 504, L131

Schunker, H., Braun, D. C., Cally, P. S., & Lindsey, C. 2005, ApJ, 621, L149

Schunker, H., Braun, D. C., Lindsey, C., & Cally, P. S. 2008, Sol. Phys., 251, 341

Woodard, M. F., & Noyes, R. W. 1985, Nature, 318, 449

Zhao, J., & Kosovichev, A. G. 2006, ApJ, 643, 1317

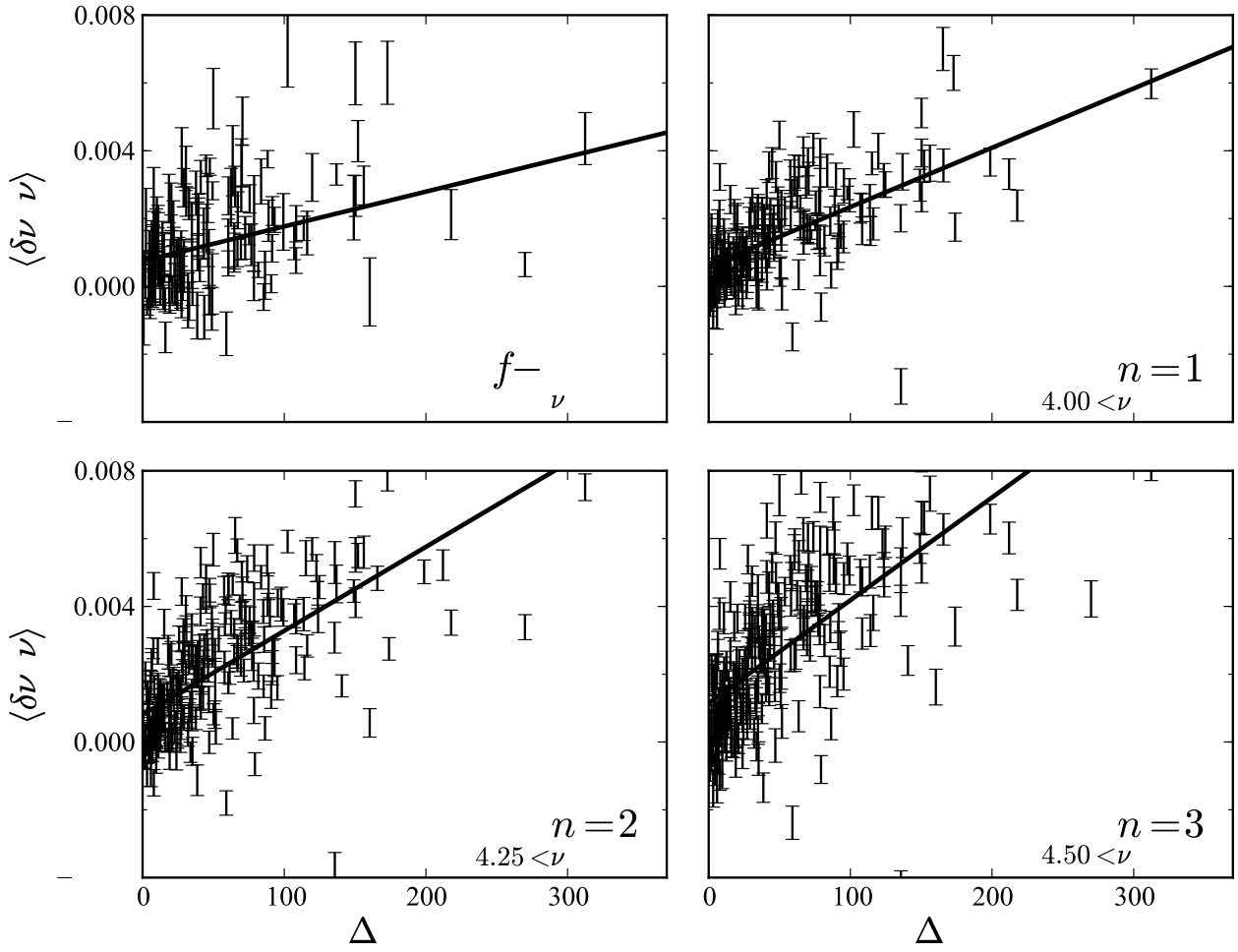

Fig. 1.— Averaged frequency differences are for the f-mode and first three p-modes, as a function of the difference in MAI. The differences are with respect to a quiet region near the active region. The range of frequencies over which the averages were taken is shown in each panel. The straight lines are the best linear fits to the data.

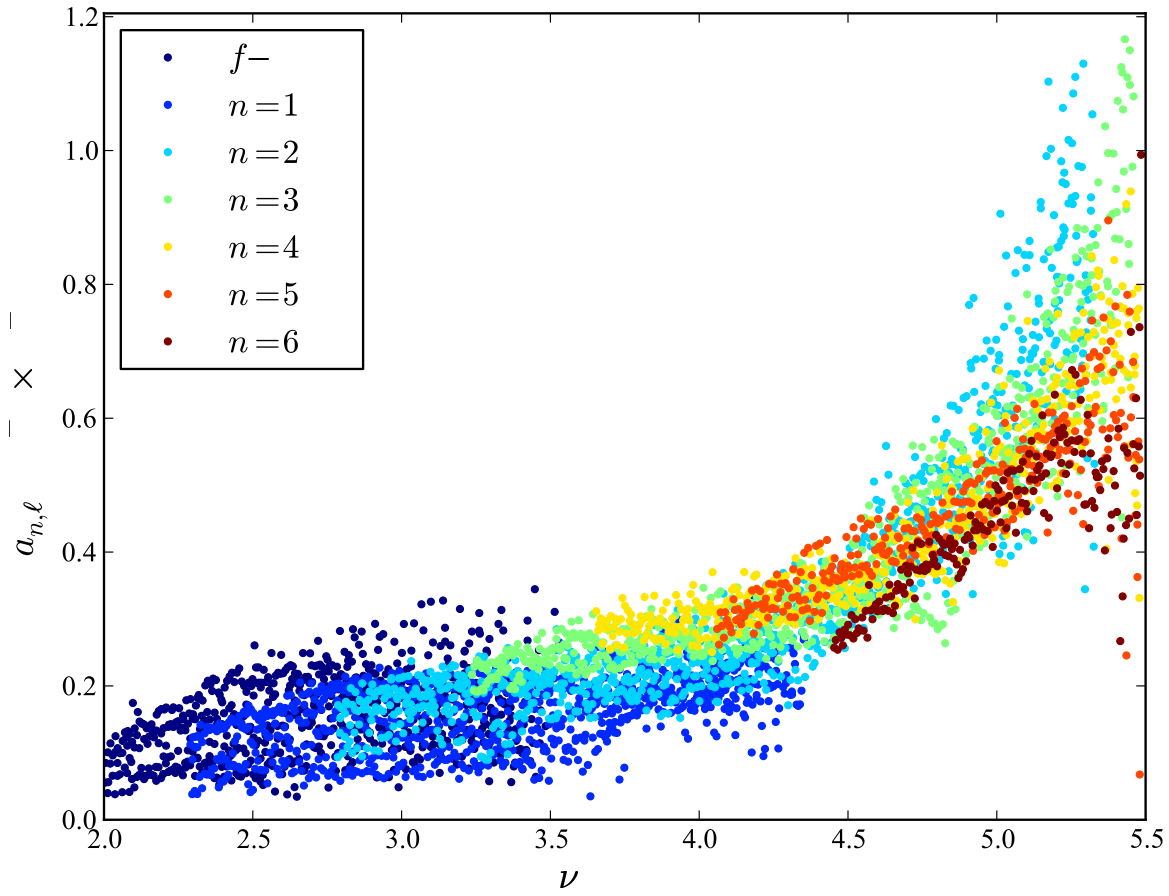

Fig. 2.— Slopes $a_{n,\ell}$ of individual mode frequency shifts with magnetic activity as a function of frequency up to $\nu = 5.5$ mHz. Different colors are used for different radial orders n.

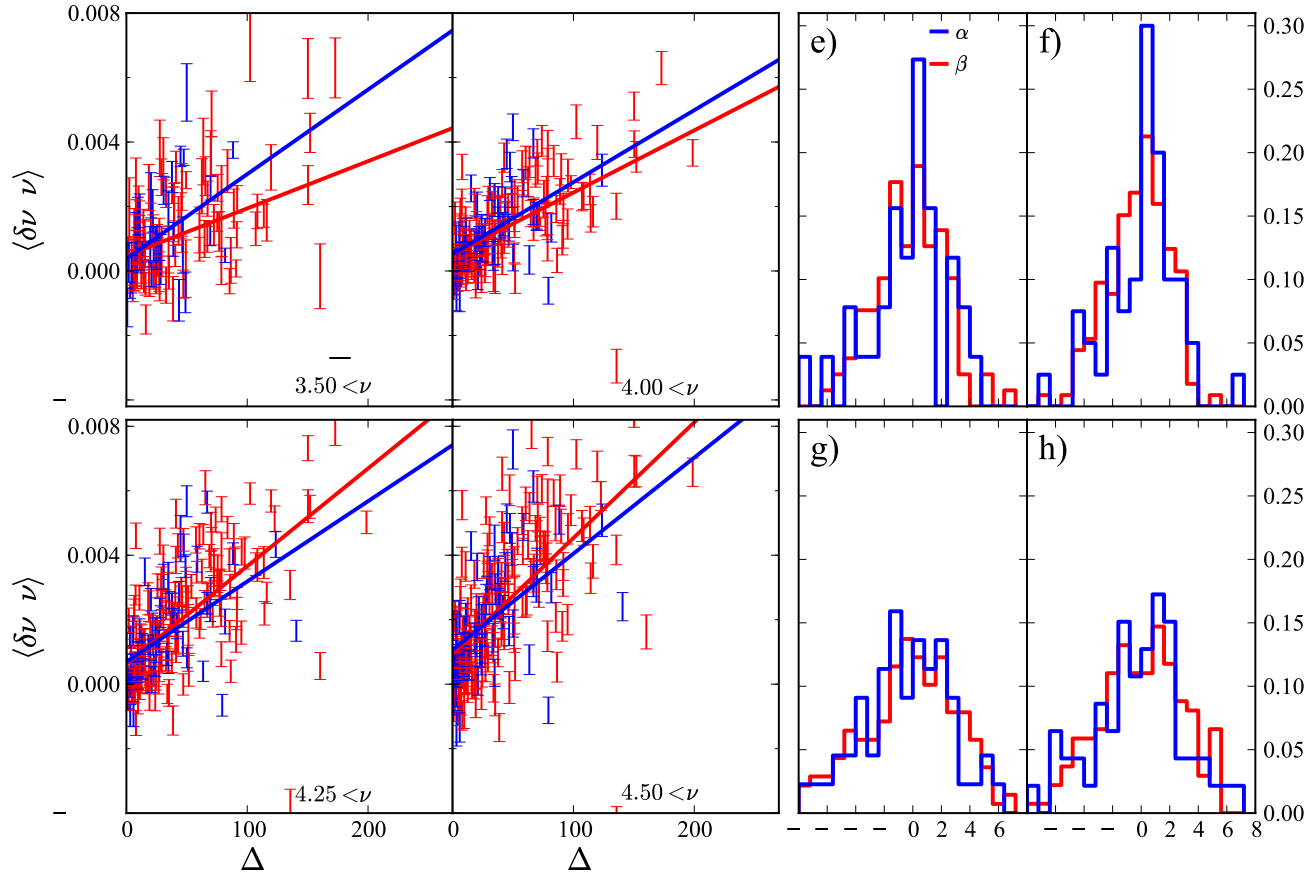

Fig. 3.— Averaged frequency differences separated by spot type for the f-mode and the first three p-modes as a function of the change in magnetic activity Δ MAI. The frequency ranges are shown in panels a) — d). Blue points denote α-type sunspots, red points denote β-type sunspots. Histograms of the residuals are also shown in panels e) — h).

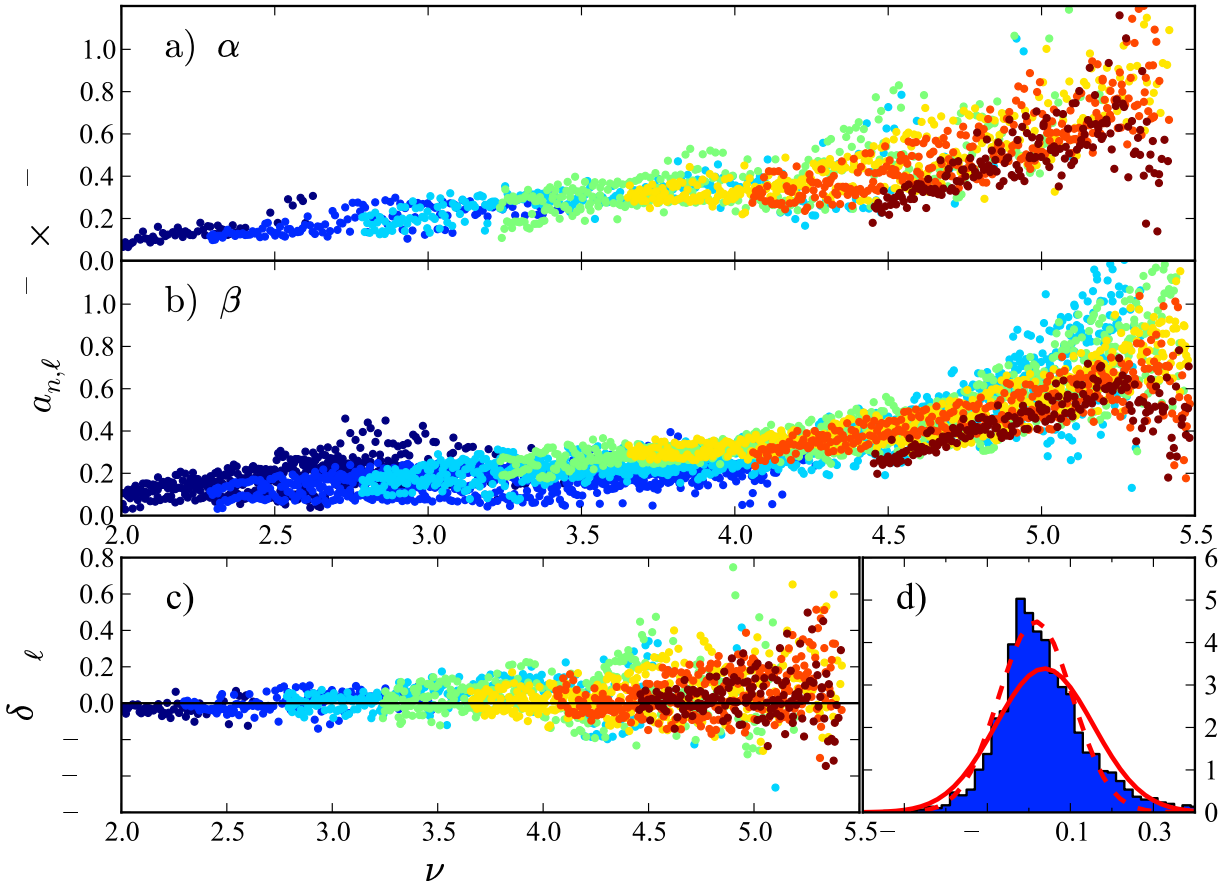

Fig. 4.— Differences in the slopes of individual mode frequency shifts with magnetic activity between α-type active regions and β-type active regions. Panels a) and b) show the slopes $a_{n,\ell}$ fit to the sample of α-type spots and β-type spots, respectively. Panel c) shows the differences $\delta a_{n,\ell}$ between the two sets of slopes. The differences are shown as a function of frequency up to $\nu = 5.5$ mHz. The sense of the difference is $\alpha - \beta$. Different colors are used for different radial orders n, and are the same as Figure 2. Panel d) shows a histogram of the differences from panel c). The solid line is the normal curve with the mean and standard deviation of the data; the dashed line shows the best fit gaussian.